Seismic Retrofit of Defective RC Beam-Column Joints

A. H. Akhaveissy[1*], Ali Permanoon[2], Moein Mirzaei[3]

Abstract

Strong earthquakes always occur in countries with seismic risk and can potentially cause multiple deaths. This study investigates the seismic vulnerability of RC beam-column connections. Generally, it is impractical to simultaneously set up the molds of the concrete beam, ceiling and column and achieve a uniform concrete and this can cause numerous constructional deficiencies. Usually, these deficiencies can be instrumental in the failure of RC frames. Therefore, this study investigates the performance of a defective RC beam-column connection and provides a method to improve the behavior of the connection. The defective connection studied herein belongs to a high school in the city of Kermanshah, Iran. Many factors that affect the performance of the retrofitting designs are studied. Also, all of the parameters used in the analyses were obtained based upon the actual behavior of the material through core extraction and tensile tests. Finally, an optimal design is proposed.

Keywords

defective connection, RC frame, retrofitting, brittle behavior of RC connections

1 Department of Civil Engineering, Faculty of Engineering, Razi University, P.O. Box: 67149–67346, Kermanshah, Iran
2 Department of Civil Engineering, Faculty Engineering, Razi University, Kermanshah, Iran
3 Advanced Numerical Calculation Center of Structural Engineering, Razi University, Kermanshah, Iran
* Corresponding author, e-mail : ahakhaveissy@razi.ac.ir

1 Introduction

One of the central constituents of reinforced concrete moment-resisting frames are the beam-column joints which are responsible for the stability of the frames when it is under the influence of seismic excitation [1, 2]. In many instances, post-earthquake inspections of structures with RC moment resisting frames damaged during earthquakes, have shown that the damage inflicted upon the frames was mostly concentrated in the beam-column joints [3–9]. Also, it has been noted that external beam-column joints are more exposed to damage compared to internal beam-column joints because of their geometrical discontinuity and subpar confinement [2, 3, 10]. While extensive studies have been carried out to enhance the quality and performance of beam-column joints, less effort has been put on addressing the practical methods through which to seismically retrofit defective beam-column joints [11]. Accordingly, the ACI-ASCE committee 352 currently recommends that "these joints need to be studied in detail to establish their adequacy and to develop evaluation codes for building rehabilitation. Methods for improving the performance of older joints need to be studied. Scarce information is available on connection repair and strengthening'' (p. 20). In the past four decades, multiple studies were performed to assess the seismic behavior of the existing reinforced concrete beam-column joints designed in accordance with different codes of various countries [12–17]. In the previous two decades, the seismic retrofitting of imperfect RC beam-column joints has been given substantial attention and multiple techniques have been proposed to seismically retrofit the reinforced concrete beam-column joints [18–25]. The goal of these studies was to improve the shear and bonding capacity of the joints to forestall brittle failure and also to ensure that beam plastic hinging would occur. Seismic retrofitting of the beam-column joint was particularly difficult in 3D frames due to accessibility limitations such as the existence of transverse beams and the floor slab adjacent to the joint area. The difficulties faced in these investigations clarified that it is important to come up with practical techniques to efficiently retrofit the beam-column joints of the existing RC structures. One of the first methods that was put forward to locally

rehabilitate non-seismically detailed RC beam-column joints was jacketing [26], regarding which multiple investigative projects were reported [18–21]. Notwithstanding, these methods of rehabilitating joints were proven to be quite costly in terms of detailing[26]. Furthermore, fastening the plates to the joints entails using either bolts that are attached to the concrete by some sort of bonding adhesive or some type of mortar-like material to seal the gap between the concrete and the plate. The introduction of Fiber Reinforced Polymer (FRP) made possible the introduction of various retrofitting methods to increase the shear strength of non-seismically detailed RC beam-column joints. A retrofitting approach that was experimentally examined by Pampanin, Christopulos [27], Said and Nehdi [28] and Sharbatdar, Kheyriddin [29], was to mount diagonal metallic haunches on the beam-column to protect the panel zone. This way of retrofitting mobilizes the part of the beam and column immediately adjacent to the panel zone of the joint and aids the joint in withstanding the shear force input which procrastinates the shear failure of the joint. The force acting on the elements framing into the joint which had to be transmitted by the joint was attenuated relocating the force flow and also by causing the plastic hinges of the beam to form at the edges of the retrofitted connection. A modelling process for bolted top-and-seat components that can be potentially used in MRFs was put forth by Brunesi et al [30]. Through a series of FE analyses and by taking into account the effects of friction, bolt pretension and the relative slippage of components, the authors were able to replicate the cyclic-reversal test protocol. To evaluate how much partially restrained (PR) bolted beam-column connections affect the overall dynamic response of MRF buildings subjected to seismic excitation, a numerical process incorporating 3D solid and 1D fibre based finite element models were constructed and verified using previous experimental data [31]. A method by the name of "planar joint expansion" was recommended by Pimanmas and Chaimahawan [19, 32] which involves broadening the shear area of the joint by using on-site cast reinforced concrete. To fasten the new concrete jacket to the beam and column, dowel bars were used in expanded joint panel area and epoxy adhesive was used to annex them to the beam and column. In 2015, Yurdakul and Avsar [33] experimentally investigated the efficacy of externally installed post-tension rods on RC beam column joints. They subjected five full-scale RC beam-column joints to cyclic loading and observed that the ultimate lateral load capacity of the retrofitted specimens rose significantly. Arzeytoon and Hosseini[34], in 2014 and using experimental models, probed the efficiency of a rehabilitation scheme composed of angles, steel plates and post-tensioning rods. The good results of the experimental study were duplicated via numerical simulation. Using three half-scale samples, Shafaei et al [35] assessed enlarging external RC beam-column joints using prestressed steel angles. All the specimens were subjected to lateral cyclic load both before and after retrofitting. In that study,

it was reported that the strength, stiffness and ductility of the damaged joints were fully recovered upon retrofitting the joint. In this research, the seismic vulnerability of a column to ceiling connection is investigated. Poorly constructed column to ceiling connections are always prone to failure and so retrofitting them is imperative. In this study, the performance of the panel zone of a poorly constructed column-ceiling connection in a high school in the city of Kermanshah in Iran was investigated. To improve the behavioral characteristics, ductility, and the strength of the connection, 9 different retrofitting schemes are proposed. Through a step-by-step approach, this study strives to evaluate how different factors influence the behaviour of a retrofitting scheme and based on the results of the performed analyses, an optimal design is introduced. This methodology can provide the engineer with a good understanding of how different parameters affect a retrofitting model. The mechanical properties of the material used in the analyses were all obtained through in-situ tests including concrete core extraction and tensile tests for the steel bars. The criteria upon which most design codes and standards (including the FEMA440 standard) assess the validity of a retrofitting scheme are the two factors of ductility and strength. When proposing every single model presented herein, it was tried to take these two factors under consideration. Also, the area beneath the load – displacement diagram represents the amount of energy absorbed by the connection. Therefore, as the two factors of ductility and strength concurrently increase, the amount of energy absorbed by the connection increases as well and this is evident from all of the models. In addition, throughout the whole study, it was tried to propose models with geometries that are easy to implement so as to inflict as less damage as possible to the structure while the retrofitting is being performed.

2 Retrofitting moment resisting connections using steel jacketing

Considering the high number of failures that occurred around or inside fillet welds connecting the beam flange to the column in moment resisting connections during the 1994 Northridge earthquake [36], the FEMA-267[37] guideline proposed a series of seismic retrofitting strategies including haunch at bottom flange, top and bottom haunch, cover plate sections, upstanding ribs, top and bottom bolted bracket, and side-plate connections. The complete designing process of this type of retrofitting which includes choosing the geometry and the stiffness of buttressing elements welded to it was proposed by Yu-Uang [38, 39]. It has to be said that the main goal of this retrofitting scheme is to move the plastic hinge away from the face of the column so as to protect the welds of the connection from premature cracks. In this study, by employing a similar idea, the behavior of a seismically designed connection that is poorly constructed was investigated and a step-by-step approach through which to retrofit the connection was introduced. Due to reasons like poor construction techniques or

inadequate vibration, the concrete of the topmost portion of the column (where the column frames into the ceiling) is defective and is of low strength and quality. Therefore, the connection was retrofitted with a steel cage and pre-stressed bolts. The pre-stressing force increases confinement in the connection, delays the formation of tensile cracks, and prevents the early failure of the honeycombed concrete near the connection.

In fact, the duty of the panel zone is to transfer the forces of the members framing into it (transferring forces from the beam to the column). In this method, by changing and adjusting the forces in the panel zone area, the location of the plastic hinge is shifted away from the connection and toward the inner areas of the beam and also a smaller portion of the total force would be placed on the column-ceiling connection. Force transferring mechanism before and after the connection is retrofitted is depicted in Fig. (1). In this retrofitting method, the external force which before the retrofitting was placed on the panel zone of the connection, is adjusted to be bore by three segments and so a smaller force is placed on the panel zone and the defective area of the column-ceiling connection.
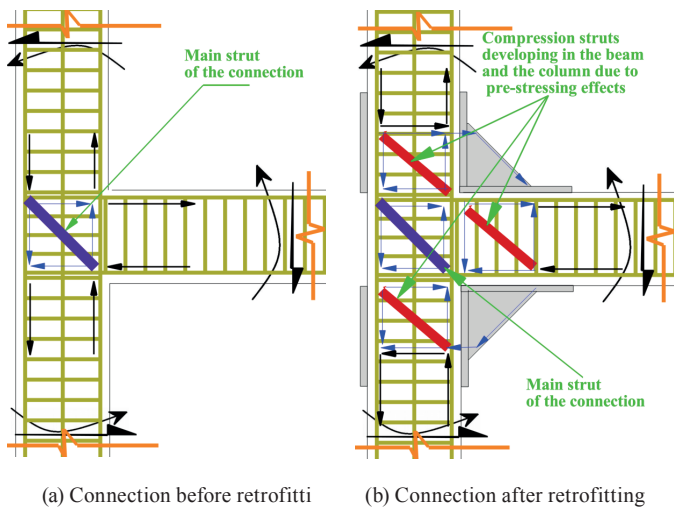
3 Deriving the mechanical properties

To obtain the mechanical properties of the concrete, a series of core extraction were performed. A total of 16 samples were taken from 3 columns and two beams (10 samples from 3 columns and 6 samples from 2 beams). Four samples were taken from the defective areas of the column-ceiling connection and 6 more samples were extracted from 2 other columns at, 1/4, 2/4 and 3/4 of their height. The remaining six samples were extracted from two beams at 1/4, 2/4 and 3/4 of their length. The

compressive strengths of the cylindrical samples taken from the columns and the beams with the diameter of 100 mm and the height to diameter ratio of one are presented in Table (1). Fig. (3) displays the poorly constructed column to ceiling connection before core extraction, a core sample and the testing procedure.

Fig. 2 Damage and rotation inflicted upon the end of the columns of a building by the 2003 Bam earthquake, Iran

Table 1 Strengths of the core samples

	Column (cylindrical strength)	3.2	Average = 3.05(Mpa)
		2.8	
		3.5	
		2.7	
Destructive test	Column (cylindrical strength)	26.4	Average = 25.5(Mpa)
		27.8	
		24.8	
		25.9	
		24.2	
		23.9	
	Beam (cylindrical strength)	24.7	Average = 25.15(Mpa)
		26.3	
		25.5	
		24.1	

Based on the carried out tests, the compressive strength of the samples extracted from the intact parts of and the defective parts were chosen to be 25 and 3 MPa, respectively. The tensile strength of the longitudinal steel bars and the stirrups used in the beams and columns is 400 MPa and are in compliance with the Russian GOST 5781-82:1993 standard. Based on the acquired data from the tests and field observations, the concrete at the upper 150 mm of the column (colored in green), is defective. The dimensions of the column of the studied connection are 500*500. Also, the beam has a height of 450 mm and a width of 400 mm. The details of the poorly constructed connection in the high school, including the dimensions and the reinforcements are depicted in Fig. (4).

(a) Connection before retrofitti (b) Connection after retrofitting
Fig. 1 Load transfer mechanism in the connection

Fig. (2) displays an obvious example of an incorrectly constructed beam-ceiling connection in Kerman province, Iran whose top section has suffered substantial seismic damage and rotation caused by the 2003 Bam earthquake. It is clear that a defective column-ceiling always threatens the stability of a structure and therefore retrofitting becomes imperative.

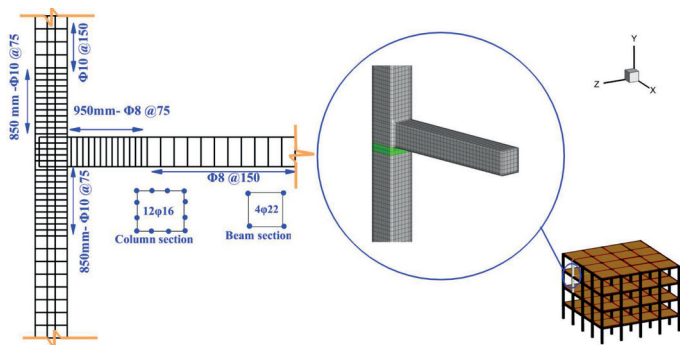**Fig. 3** View of the poorly constructed connection and the core extraction operation

Fig. 4 Dimensions and the reinforcements of the connection

4 Numerical simulation

The finite element commercial software ANSYS was used for the numerical simulation. To model the behavior of the concrete, the eight-node, three dimensional SOLID65 element with 3 degrees of freedom in each node was employed. To model the nonlinear behavior of the concrete, the Willam-Warnke [40] yield criterion was used. In 2-D space, the principal stresses in this failure surface are as follows:
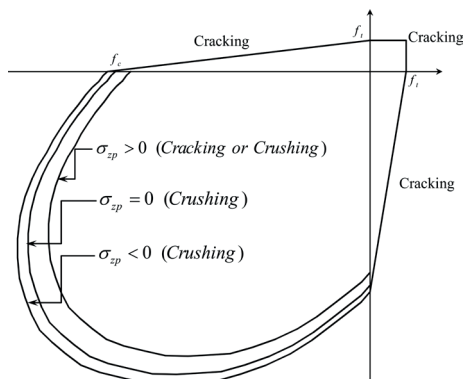
Fig. 5 Willam-Warnke yield surface in 2D space

It has to be mentioned that this yield surface has the ability to take into account the crushing effect in compression and cracking is tension. It is noteworthy, also, that the behavioral model employed for the concrete assesses the cracks in the principal planes and in the Gauss points [40]. Thus, considering the positioning angles of the principal planes in 3D space and in each Gauss point, the model is capable of accounting for lateral cracks. Therefore, if a fine enough mesh is used in the simulation, these cracks are merged in the Gauss points and the paths of the lateral cracks can be modelled. A good example of evaluating the lateral crack effect can be found in the work done by Brunesi and Nascimbene [42] where a good agreement was seen between the results of the numerical model and the experimental observations. Also, to model the behavior of the steel plates, the eight-node, three dimensional SOLID45 element with 3 degrees of freedom in each node was utilized. Further, the Von Mises yield surface was used to model the nonlinear behavior of the steel material. The friction between the concrete and the steel plates was accounted for using the contact elements CONTA174 and TARGET170 and the Mohr–Coulomb yield surface was used to model the frictional behavior. The friction coefficient was considered equal to 0.5.[43]

Based on multiple tests on cylindrical concrete samples, Hognestad proposed the following equation to describe the behavior of concrete in compression:

$$f_c = f_c' \left[2 \left(\frac{\varepsilon}{\varepsilon_0} \right) - \left(\frac{\varepsilon}{\varepsilon_0} \right)^2 \right] \tag{1}$$

In the numerical modelling, this equation was used to model the compressive behavior of the concrete. Also, the following diagram presents the stress–strain curve used for the concrete in tension. The tensile relaxation (softening) was presented by a sudden reduction of the tensile strength to $0.75 f_t$ upon reaching the tensile cracking strain (ε_{cr}). After this point, the tensile response decreases linearly to zero stress at a strain of $6 \varepsilon_{cr}$ (Fig. 6).
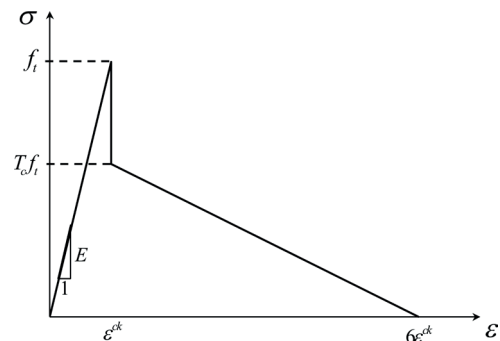

Fig. 6 Tensile behaviour of the concrete

Now, numerically modelling a cylindrical concrete sample (pictured below) can furnish the necessary information to draw a comparison between the mathematical relationship and the numerical analyses.
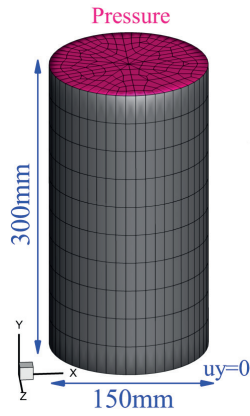
Fig 7 Finite Element modelling of the concrete cylindrical sample

As it can be seen from Fig. 8-a, there is a very good agreement between the mathematical model and the numerical simulation:
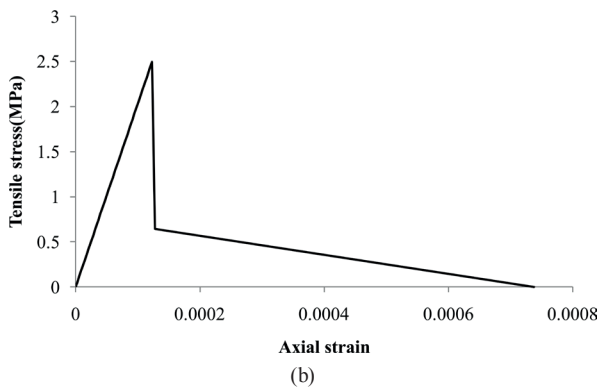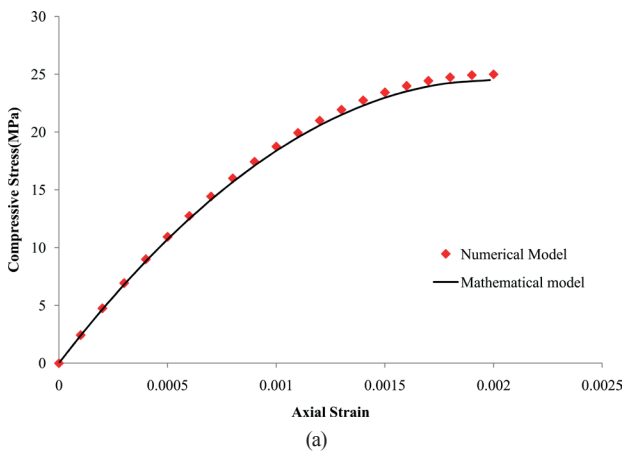

(a)

(b)

Fig 8 (a) The compressive stress of the mathematical and numerical models and (b) response of the Finite Element cylindrical sample

Thus, it is safe to assume that the abovementioned elucidations can theoretically corroborate the authenticity of the numerical models.

To verify the parameters used in the software and also to ensure the correct performance of the numerical model, the beam-column connection studied by Shafaei et al [27] (the C1 model), which in terms of concrete strength, reinforcement and geometrical properties is almost similar to the reference model of this study, was used. The geometrical properties of the model by Shafaei et al [27] and also the simulation carried out in the ANSYS software are presented in Fig. (9).
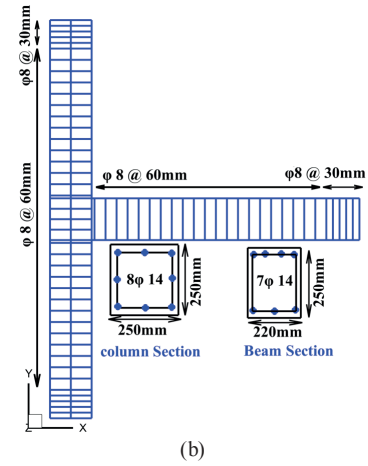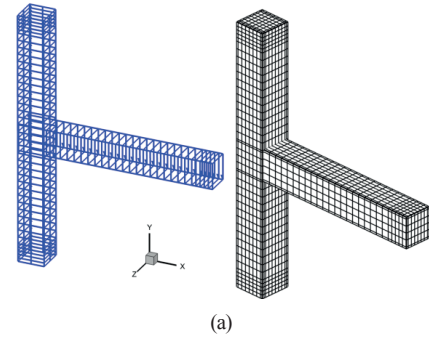

(a)

(b)

Fig. 9 (a) The steel reinforcement (left) and the Finite Element mesh (right) (b) the experimental model (the C1 model)

By comparing the load-displacement diagram of the C1 model and its simulation in the ANSYS software using the obtained parameters, a good agreement can be seen (Fig. 10). Also, by assessing the developed cracks in the experimental and the numerical models, it can be ensured that the failure modes of the two models match (Fig. 11). In this study, by keeping the strength parameters of concrete and steel constant, the retrofitting of the poorly constructed connection is investigated.
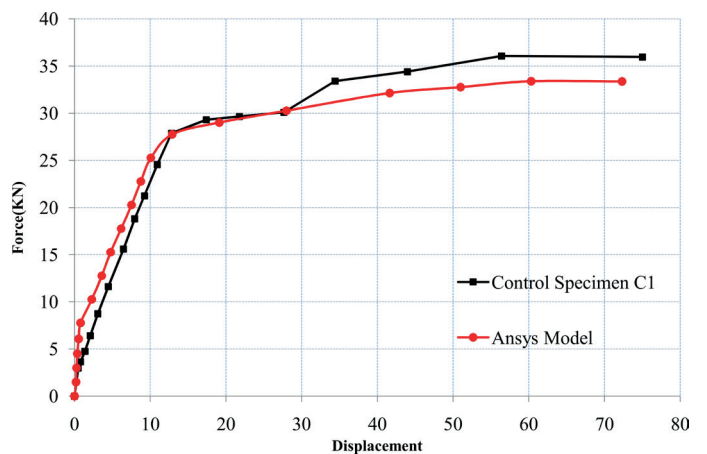

Fig. 10 Load-displacement diagrams of the C1 model and the finite

To numerically model the poorly constructed connection and also to propose retrofitting schemes, the strength values of the material were obtained through tests and are given in Table (2). These parameters were employed and kept constant in all the numerical models.
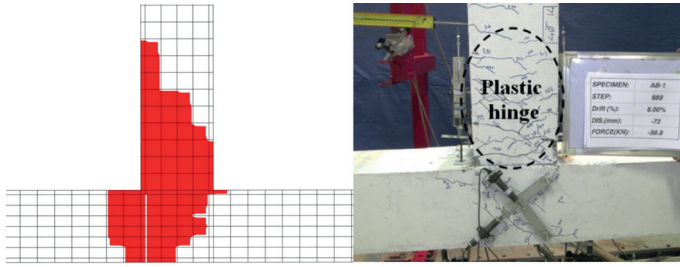
Fig. 11 Crack development pattern in both the experimental and the numerical models

Table 2 The mechanical specifications of the material

Different materials	Tensile strength (MPa)	Compressive strength (MPa)
Concrete	2.5	25
Defective concrete	0.3	3
Steel plate	240	240
Bolt	420	420
Steel bars	400	400

5 Analysis and assessing the results

To model the connection, half of the upper and lower columns and also half of the beam framing into the connection were modeled. The modeling procedure, the meshing, the configuration of the reinforcement, the supports and the geometrical properties of the reference model and also the applied loads and moments are illustrated in Fig. (12). To model the behavior of the defective area of the concrete, the concrete strength of this area was considered to be 3 MP
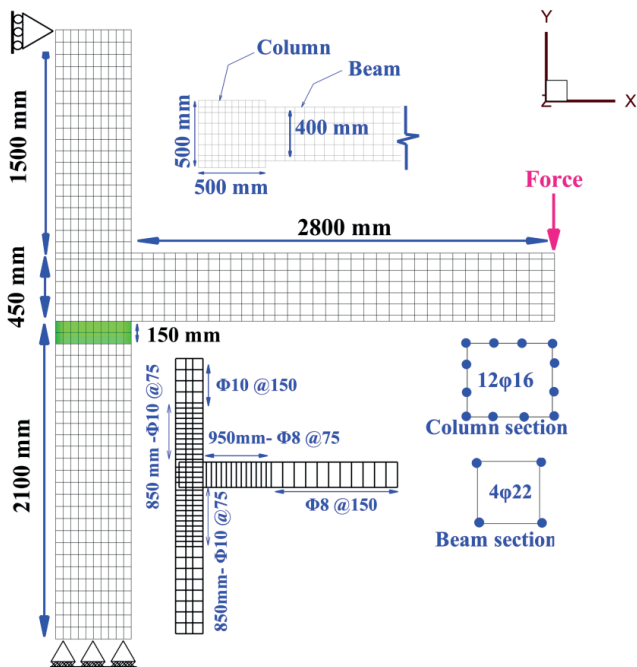

Fig. 12 The details and dimensions of the beam and column and the load mechanism

By carrying out the nonlinear static analysis on the imperfect connection and analyzing the results, it was revealed that the connection fails at the weak point before the structure reaches its maximum capacity. The load-displacement diagram of the connection signifies its brittle behavior (Fig. 13-a). Considering the plastic tensile and compressive strains of the defective concrete at point A in the load-displacement diagram, it can be seen that the concrete is destroyed at the compressive area and cracks in the tensile area have clearly expanded. At point B in the load-displacement diagram, considering the plastic compressive strains, it can be observed the concrete of the defective area has been completely destroyed and this causes the longitudinal steel bars to buckle and the connection to lose its load bearing capacity. Thus, point B was taken into account as the ultimate capacity of the connection (Fig. 13-b).
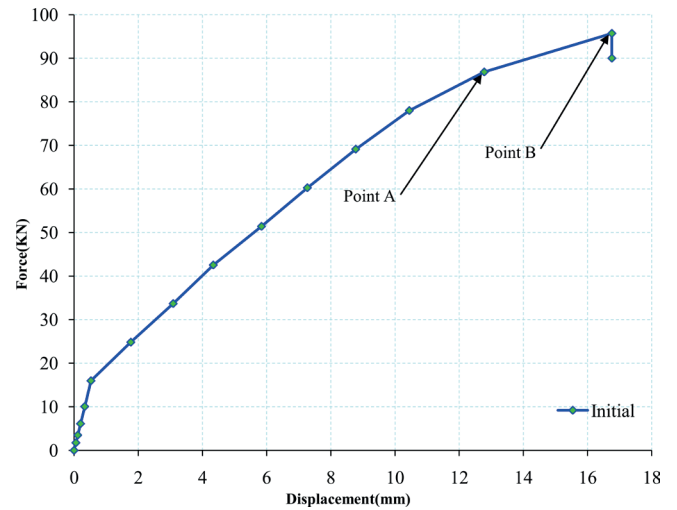
(a)
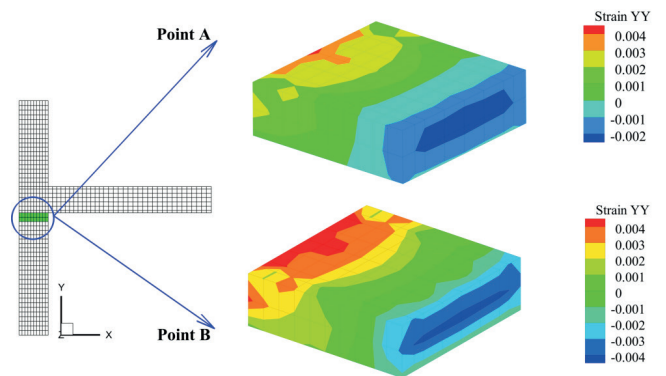
(b)

Fig. 13 (a) The load-displacement diagram of the imperfect connection; (b) The strain of the defective part at points A and B at the final moment of load carrying

As it can be concluded, retrofitting the connection seems imperative. To achieve the most suitable retrofitting model, 9 different models were investigated. Given that in retrofitting a connection, ductility, strength, and low cost and damage to the structure are always of significance, these factors have been taken under consideration in the 9 proposed retrofitting designs. The tensile bolts used to connect the steel plates to each other in the proposed models are of type A325 and according to the ASTM-A325 code, have been pre-stressed equal to either 40 or 70 percent of their yield stresses. Considering the fact that most of the details of the retrofitting models are the

same, the common specifications of the models are depicted in Fig. 14. The remaining details are given in the sections in which each model is described. The mechanical properties of all the models are identical and are tabulated in table (3).
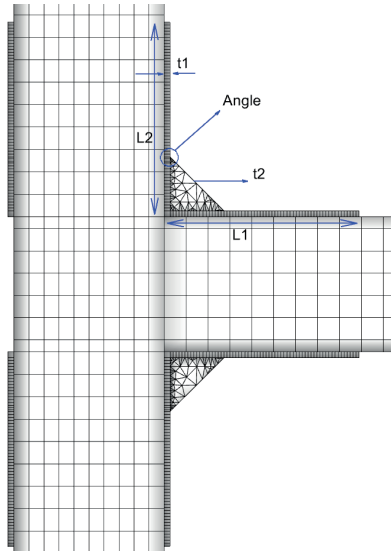

Fig. 14 The overall view of the reinforcement

6 Retrofitting Models
6.1. Model 1

The first approach to overcome the said problem is to place steel plates with the length of 450 mm, a width equal to those of the beams and columns and a thickness of 10 mm. The aims of setting up the plates are increasing the confining stress of the concrete and redistribute the developed forces in the panel zone and transferring them to the steel plates. Therefore, the plates are conjoined together using B1 to B6 bolts that have the diameter of 20 mm and are pre-stressed equal to 40 percent of their yield stresses (Fig. 15). For the bolted systems, considering that first the column and the beam are drilled, the

bolts are then placed in the drilled holes and finally concrete adhesive is used to uniformize the hole, the bolts, and the concrete. To simulate this process, the element's birth and death methodology has been employed. In the first stage of loading, the elements in the drilled hole were set to the death state and then pre-stressing is applied to the bolt. In the second step, these elements are made alive and then the loading continues. Through this approach, the construction procedure of the retrofitting is adequately modelled. Three-dimensional link elements were used to model the bolts. These elements are capable of taking into account axial force and given that bolts with a diameter of 20 mm are not expected to withstand bending, the bolts are therefore considered not to bear bending.
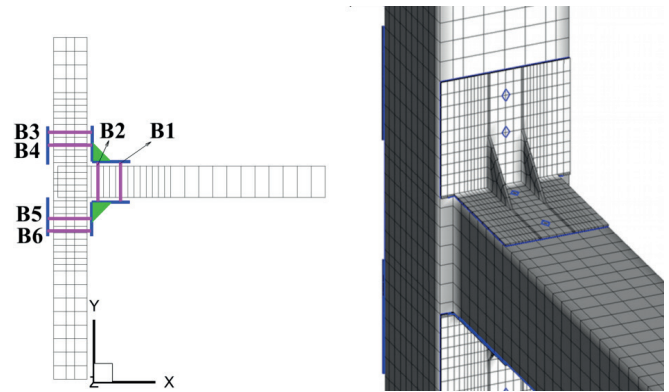

Fig. 15 The overall view of model 1 and the configuration of the steel bars, the reinforcing plates and the tensile bolts

The triangular stiffeners shown in Fig. 16 are used to stiffen the connection and redistribute the developed forces from the confined concrete to the steel plates. The dimensions of the triangular stiffeners are 10*200*200 mm. As it can be seen from the results of the Push-over analysis given in Fig. 16, the ductility of the model has increased and the brittle behavior of the connection has improved.

Table 3 The overall specifications of the reinforcing models

|	L1 (mm)	L2 (mm)	t1 (mm)	t2 (mm)	Angle (degree)	Inside Bolt of Column(d mm)	Inside Bolt of Beam(d mm)	Inside Bolt of Beam(d mm)	outside Bolt of Column (d mm)	outside Bolt of Beam (d mm)	percent of prestressing (inside Bolt)	percent of prestressing (outside Bolt)
Model(1)	450	450	10	10	45	2 (20)	2 (20)		-	-	40	-
Model(2)	450	450	10	10	45	2 (20)	2 (20)		-	-	70	-
Model(3)	450	450	10	10	45	2 (18)	2 (18)		-	-	70	-
Model(4)	450	450	10	10	45	-		-	3 (14)	3 (14)	-	-
Model(5)	450	450	10	10	45	2 (18)	2 (18)		3 (14)	3 (14)	70	-
Model(6)	450	450	10	10	45	2 (18)	2 (18)		3 (14)	3 (14)	70	70
Model(7)	950	950	10	10	45	4 (18)		-	4 (14)	5 (14)	70	
Model(8)	450	450	20	10	22.5	2 (18)	2 (18)		3 (14)	3 (14)	70	70
Model(9-a)	650	650	20	14	45	2 (18)	2 (18)		3 (14)	3 (14)	40	-
Model(9-b)	650	650	20	14	45	2 (18)	2 (18)		3 (14)	3 (14)	70	-
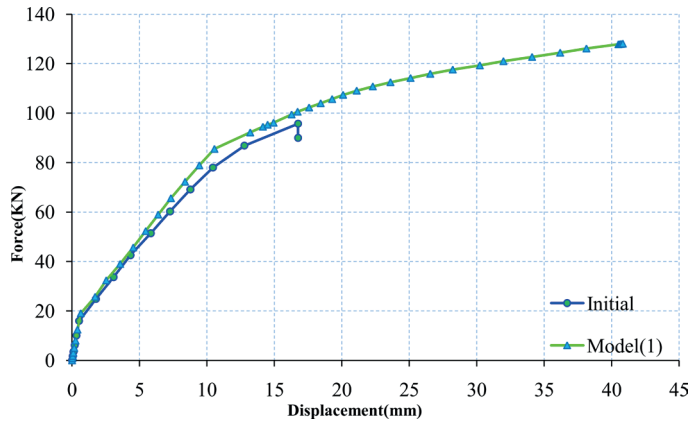
Fig. 16 Load-displacement diagram of model 1

By observing the normal stress at the final moment, it is revealed that the failure of the connection has occurred at the front of the column. Videlicet, the location of the plastic hinge is in the front of the column which is not desirable and the expansion of the tensile cracks and the crushing of the concrete of the face of the connection at the final moment confirms this assertion.

Correspondingly, by observing the Von Mises stress distribution of the reinforcing plates at the final moment, it can be seen that the maximum capacity of the steel plates has not been employed. This is probably due to the fact that the edges of the steel plates are not attached to each other, but at the location where the steel plates are connected by tensile bolts, the plates have fully contributed to stress transfer. From these results, it becomes clear that the steel plates should, at all points, be connected to each other so that they can participate in stress transfer and confining the concrete of the connection.

It has to be mentioned that the bolt is pre-stressed equal to 40 percent of its yield stress and it has a diameter of 20 mm. The force in the bolt is equal to 52778 N. The pre-stressing in the bolt has caused stress concentration in the area of the plate where the bolts is present has penetrated the concrete and the areas away from the bolt, the plate has separated from the concrete. So, assuming that the pre-stressing affects a 200*200 mm area, the average applied pressure was obtained to be 1.3 MPa. By investigating the stress distribution induced by the pre-stressed tensile bolts on the beam and the column, the contact elements are properly transferring the compression caused the pre-stressing (Fig. 18).
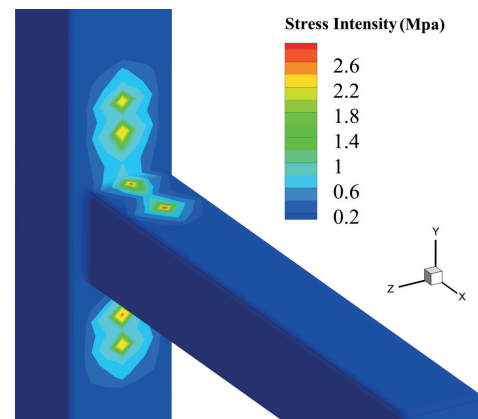

Fig. 18 Stress distribution on the concrete caused by pre-stressing of the bolts at the location where the bolts are connected to the plates
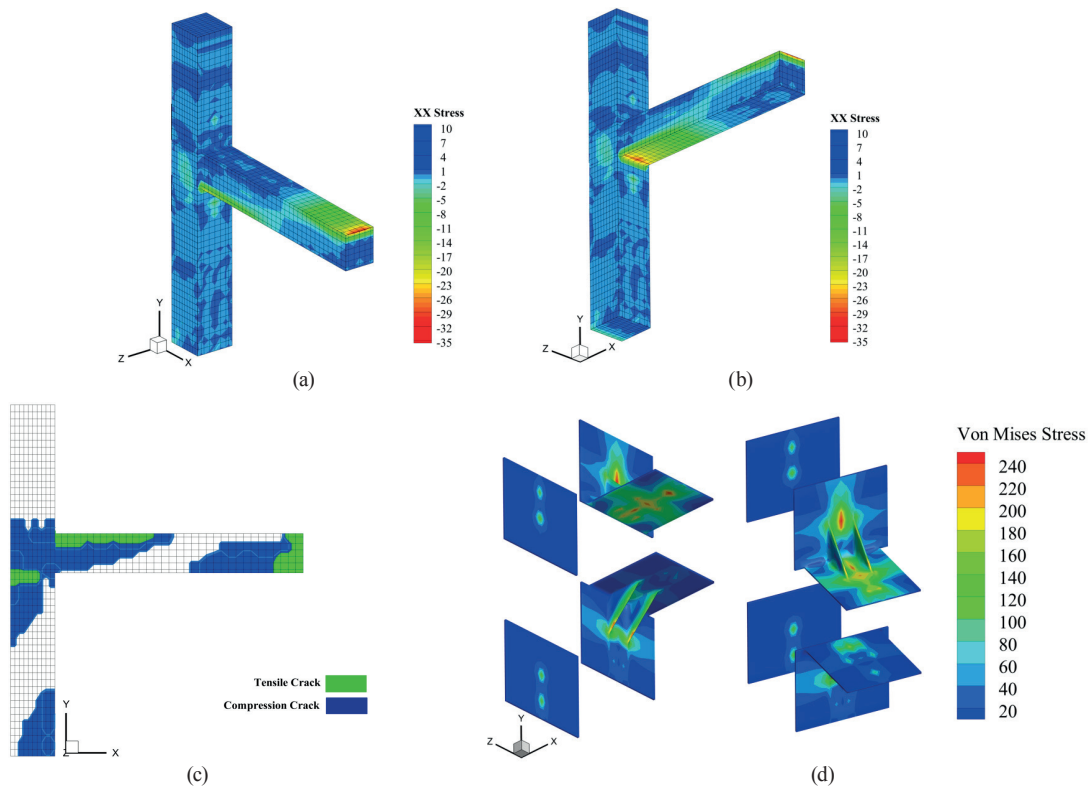

Fig. 17 (a) Normal stress on the beam at the final moment, (b) Normal stress under the beam at the final moment, (c) Expansion of the cracks at the final moments, (d) Von Mises stress distribution on the plates at the final moment

By evaluating the ultimate stress developed in the tensile bolts of the plate, it can be observed that the bolts are far from achieving their maximum capacity. In the table below (table 6), the maximum stress of the bolts B1 to B6 are presented.

Table 4 The ultimate stresses of the tensile bolts

Bolts	B1	B2	B3	B4	B5	B6
Maximum Stress (MPa)	158.4	237.91	144.5	174.9	140.1	152.7

In bolt 2, due to slippage and separation of the steel plate from the concrete, stress has increased. But the bolts are still a long way from failure. Given the fact that the whole capacity of the plates and the tensile bolts have not been used, it is possible to utilize the optimum capacity of the plates and the bolts by increasing the initial pre-stressing of the bolts. Thus, in model 2, the pre-stressing of the bolts was increased from 40 percent to 70 percent of the bolt's yield stress. Other specifications of model 2 are similar to those of model 1. Similar to model 1, in model 2, the maximum capacity of the bolts has not been employed and the bolts are able to resist load until they reach their maximum stress. Therefore, in model 3, the diameter of the bolts has been reduced from 20 mm to 18 mm. It needs to be mentioned that this change reduces costs, optimizes material usage and it also prevents the drilling of a bigger hole in the concrete. The diagrams shown in Fig. (19) illustrate the load-displacement diagrams of models 1 through 3. It's worth noting that model 3 was compared with three different pre-stressings of 40, 55 and 70 percent so that the effect of the initial pre-stressing can be assessed. By increasing the pre-stressing of the bolts at the location where the bolts are connected to the column, stress concentration happens which brings about local stresses and low ductility.
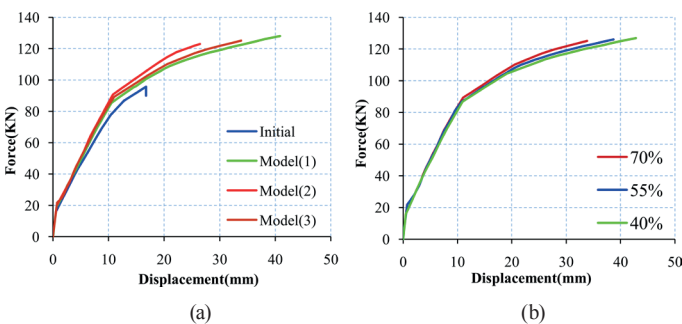

Fig. 19 (a) Load-displacement diagrams of models 1–3; (b) Model 3 different initial pre-stressings

By assessing the separation of the plates in model 2, it can be seen that the initial pre-stressing of the bolts causes the plates to penetrate the concrete at the location of the bolts and separate from the concrete in other locations and this causes the plate not to perform desirably. So, the separation of the plates at the edges has to be also sufficiently controlled. In the next model, this objective is met (Fig. 20).
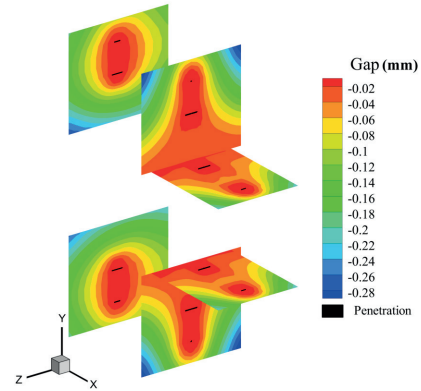

Fig. 20 Separation and penetration contour of the plate at the final load carrying

6.2 Model 4

In this model, in order to prevent the separation of the steel plates from the concrete, especially the separation of the corners, it was decided to omit the medial bolts so that only the effect of the friction between the steel plates and the concrete and also the effect of the un-prestressed side bolts can be investigated. The steel plates on the column and the beam were annexed to each other using 3 bolts with the diameter of 14 mm and no pre-stressing. The location of the side bolts are shown in Fig. (21).
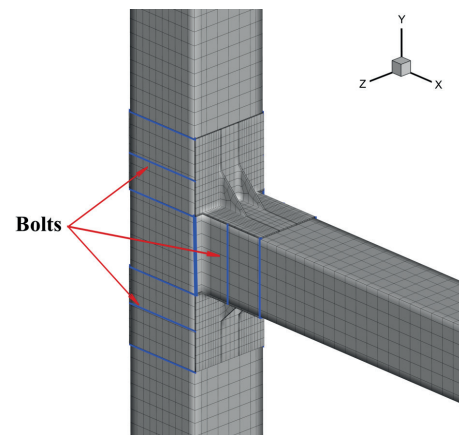

Fig. 21 View of model 4 and the placement of the side bolts

After applying the load and controlling the separation of the plates from the concrete, it is observed that the plate does not separate from the concrete at the edges. However, it does occur in the middle section. Fig. (22). So, the simultaneous use of both side and medial bolts will probably prevent the separation of the plates and causes the reinforcement to perform suitably. In model 5, the medial bolts were pre-stressed equal to 70 percent of their yield stresses and the side bolts were not pre-stressed and the performance of both types of bolts was investigated. Fig. 24 presents a comparison between the load-displacement diagrams of models 3, 4 and 5. In model 5, one can easily note that the simultaneous utilization of medial and side bolts has quite effectively increased the ductility of the connection.
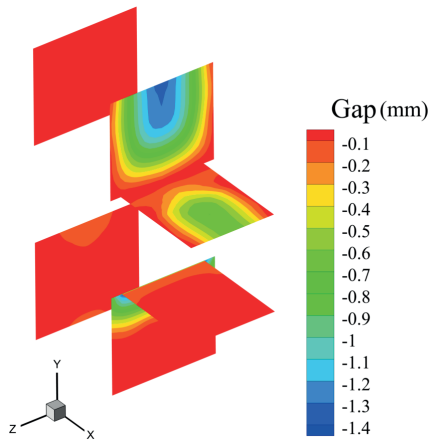
Fig. 22 Separation cantor of the plate from the concrete in model 4 at the moment when the connection reaches its final strength
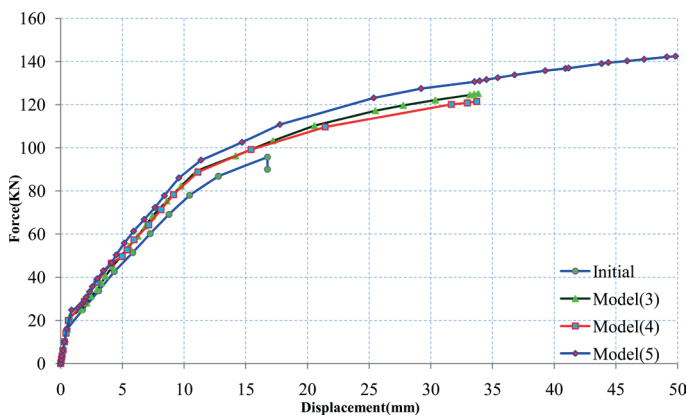

Fig. 23 Comparison between the load-displacement diagrams of models 3, 4 and 5

In model 5, by assessing the critical stress of the side bolts, of which the maximum stress is 78 MPa, it is revealed that the bolts are far from reaching their maximum capacity. Therefore, it is possible to arrive at more suitable results by pre-stressing the side bolts and increasing the confinement stress. Model 6 was constructed to take into account these two factors. In this model, in addition to the medial bolts, the side bolts were also pre-stressed equal to 70 percent of their yield stress. By comparing the load-displacement diagrams of models 5 and 6, it is obvious pre-stressing the side bolts has increased the initial stiffness and the confinement stress of the connection (Fig. 24).
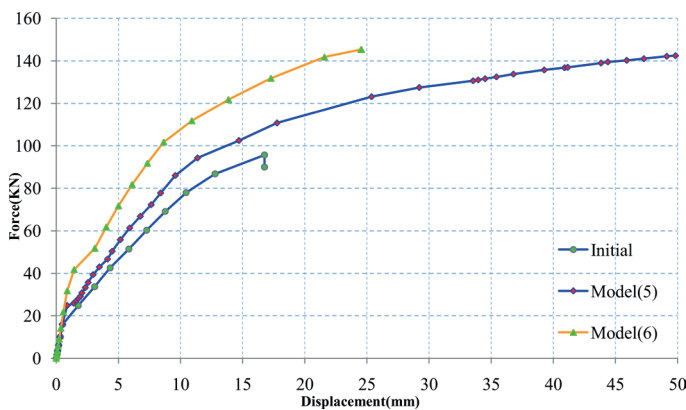

Fig. 24 Comparison between the load-displacement diagrams of model 5 and 6

Increasing the initial stiffness of model 6 has decreased its ductility. By comparing the separation patterns of the steel plate from the concrete in models 5 and 6, it was concluded that simultaneously pre-stressing the side and the medial bolts has caused the plate between them to separate from the concrete and as a result, the uniformity of the friction stress between the plate and the concrete has decreased which in turn has caused the connection to have a brittle behavior. By pre-stressing the side bolts, the concrete covering acts as a support and at the moment the load is applied, it causes the plate between the side bolt and the medial bolt to separate from the concrete. G. Santarsiero et al [41] have also used tensile straps to connect steel plates to beams and columns. The strength of the connection was increased by relatively 95 percent but the initial stiffness did not change at all which probably is due to the use of tensile straps whose presence has caused the support-like role of the concrete covering and also has caused the mid-section steel plate to separate from the concrete (Fig. 25).
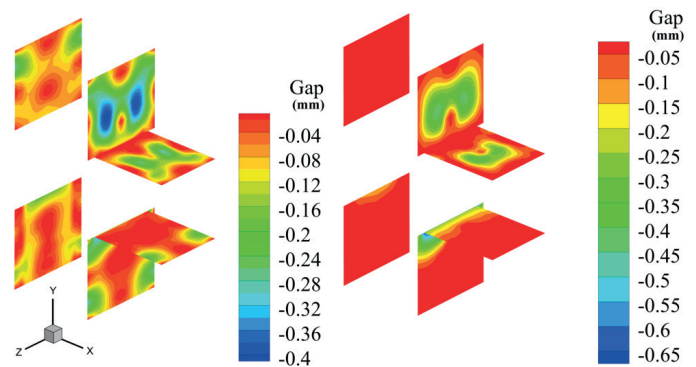

Fig. 25 Comparing the separation pattern of steel plates from the concrete at the final moment in models 5(a) and 6(b)

In this model, by investigating the plastic strains and the expansion of the cracks, it was observed that the location at which the cracks started developing is the front of the column which is not desirable. Therefore, it is possible to drive the location of the plastic hinge away from the column and into the beam by increasing the length of the plate.

6.3 Model 7

In this model, to level out the transitive stress between the plate and the concrete and also to drive away the plastic hinge from the column and moving it into the beam, plates with the length of 950 mm and the thickness of 10 mm were used. The reinforcing plates were attached to the beam using 5 un-pre-stressed side bolts. To connect the plate to the column, 4 medial bolts pre-stress equal to 70 percent of the bolts' yield stresses and 4 un-prestressed side were used. The reason behind using the medial bolts is to increase the confinement in the column and in the defective area.
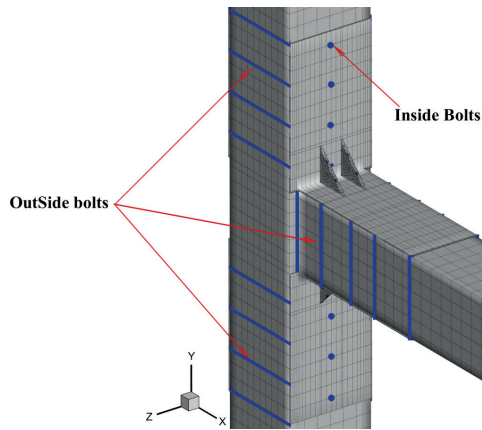
Fig. 26 View of model 7 and the placement of the bolts

By comparing the load-displacement diagrams of model 5 and 7, it can be seen that model 7 demonstrates a higher initial stiffness and carries more load. However, compared to model 5, its ductility has diminished which probably is due to the absence of medial tensile bolts in the beam. Fig. (27). Therefore, for the concrete to perform desirably and have sufficient confinement stress, it is necessary to use tensile bolts in both the beam and the column simultaneously.
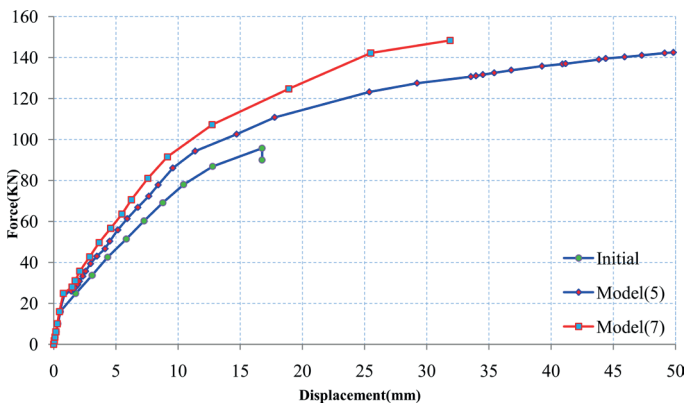

Fig. 27 Comparing the load-displacement diagrams of models 5 and 7

Considering the Von Mises stress contours on the steel plates at the final step, it can be seen that the ending 300 mm of the steel plates do not have a significant share in carrying the applied loads. The stresses change over the range of 0 to 30 MPa. Thus, it would financially sound to remove the ending 300 mm of the plates. Fig. (28). In model 9, the dimensions of the plate will be decreased to 650 mm.

6.4 Model 8

In model 8, to uniformly distribute the stress resulted from the pre-stressing of the bolts, transverse stiffeners with the dimensions of 10*50 were used. It has to be mentioned that the length of the reinforcing steel plates in this model is 450 mm. The medial bolts in this connection have a diameter of 18 mm and the side bolts have a diameter of 14 mm. Both bolt types have a pre-stressing of 70 percent of their yield stresses. In this model, to increase ductility, the angle of the triangular stiffeners has been decreased from 45 degrees to 22.5 degrees. Fig. (29).
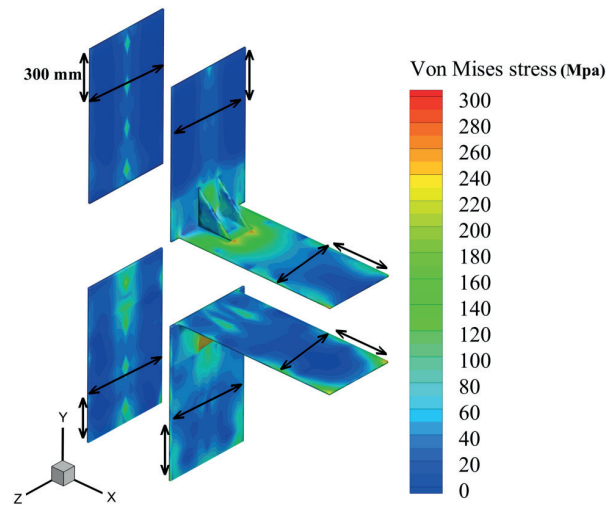

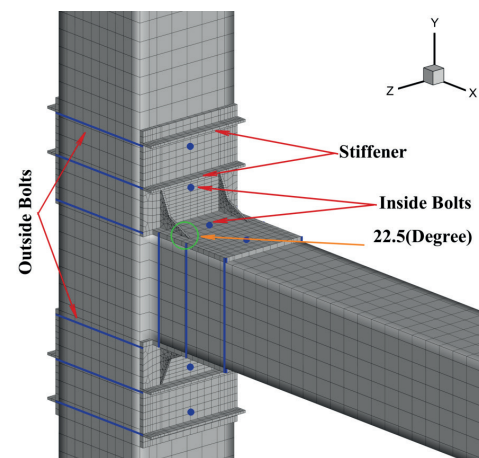**Fig. 28** Von Mises stress distribution of the reinforcing plates at the final moment

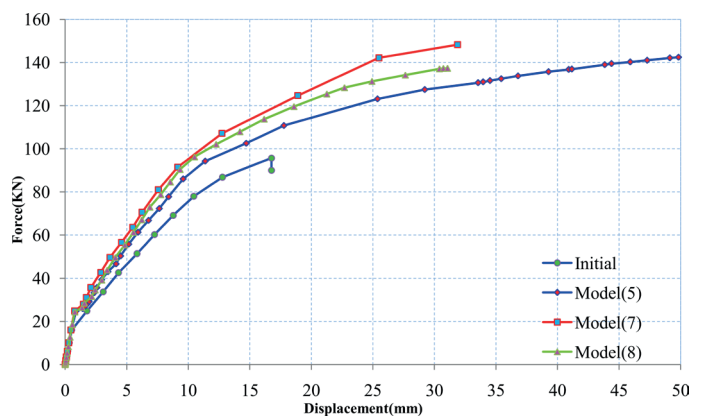**Fig. 29** View of model 8 and the placements of the bolts and the stiffeners

Fig. 30 Camparing the load-displacement diagrams of models 5, 7 and 8

By comparing the load-displacement diagrams of models 5, 7 and 8, it can be deduced that in this model, the initial stiffness increases due to the presence of the stiffeners. However, at the end of the loading process, the stiffness and the ductility of the connection decreases. Fig. (30). This decreasing trend originates from 2 distinct factors: First is the reduction of the angle of the triangular stiffeners and second is the support-like behavior of the concrete covering resulted from the side bolts

being pre-stressed which brings about the local failure of the concrete covering and also weakens the confinement of the concrete. Even by increasing the number of the transverse stiffeners, the support-like effect of the side bolts cannot be reduced. Hence, for the side bolts not to have a reducing effect, they need to be either removed or be replaced with straps.

The second factor is the reduction of the angle of the triangular stiffeners which by observing the Von Mises stresses on the plates, it can be seen that triangular stiffeners have yielded before they reached their ultimate capacity and this accelerates the reduction of the connection's initial stiffness. It needs to be noted that the presence of transverse stiffeners almost keeps the separation of the steel plates from the concrete under control and transfers the stresses caused by the friction between the steel plates and the concrete in a uniform manner (Fig. 31).
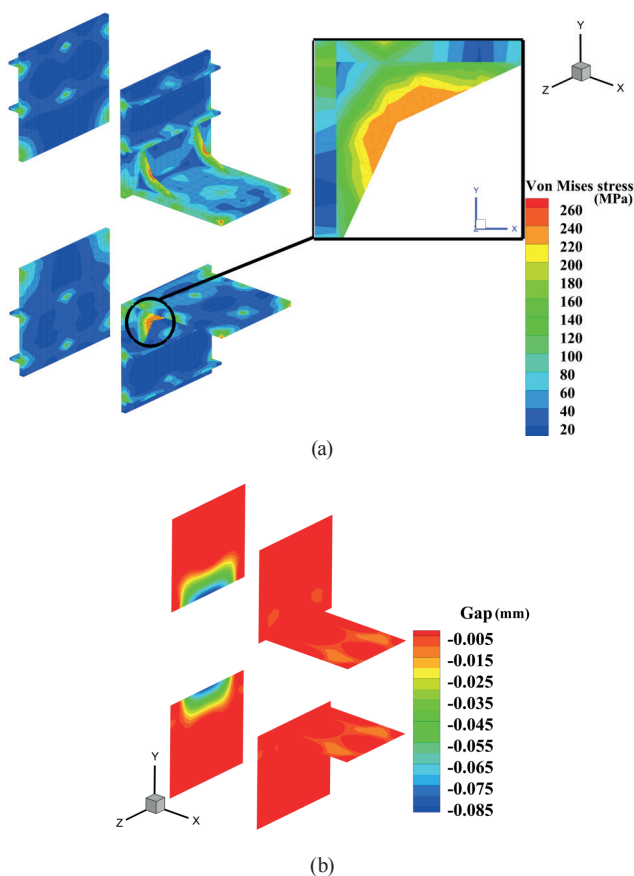

(a)

(b)

Fig. 31 (a) Von Mises stress contour in the plates and the triangular stiffeners at the final moment; (b) Separation of the steel plates from the surface of the concrete at the final moment

6.5 Model 9

Model 9 is combination of all the previous models. Based on the results from model 7, the length and the thickness of the plate in this model are 650 mm and 20 mm, respectively. Based on the results from model 8, the angle of the triangular stiffeners is 45 degrees and the number of the transverse stiffeners on the column is 3 on each side. The number of tensile bolts on the beam and the column is 2 and their diameter is 18 mm. In models 9-a and 9-b, the bolts have been pre-stressed equal to 40 percent and 70 percent of their yield stresses,

respectively. Considering that the pre-stressings of the side bolts cause local failures, straps with the width of 50 mm have been used in place the side bolts to annex the reinforcing steel plates together. The straps are placed based on the position of the joists that are placed perpendicular to the beam so that when the retrofitting is being performed, as little damage as possible is inflicted upon the ceiling. Fig. (32).
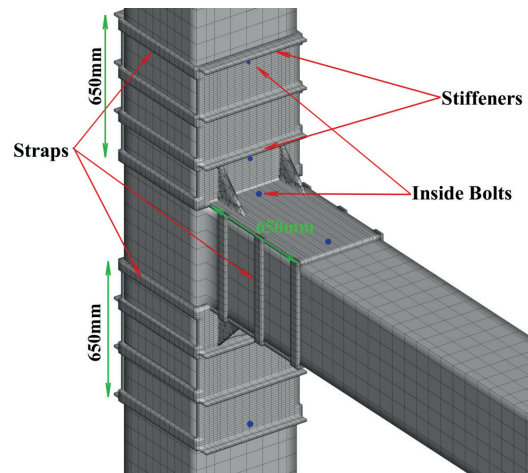

Fig. 32 View of model 9 and the placement of the straps and the bolts

By comparing the load-displacement diagram of model 9 to those of the other models, it can be seen that both the ductility and the load bearing capacity of the connection has considerably increased and therefore this model is a suitable choice with which to retrofit the connection. Using straps instead of pre-stressed side bolts has brought about a more ductile behavior and has barred the steel plates to separate from surface of the concrete which was due to the support-like behavior of the pre-stressed side bolts. It should be noted that the use of straps instead of pre-stressed side bolts prevents the development of local stresses in the concrete covering and the confinement behavior of the concrete is also more effective. Moreover, compared to model 7, more optimized steel plates have been used in this model which in practice has the benefit of destroying a smaller portion of the ceiling at the time of retrofitting. Model 9-a, whose bolts are pre-stressed equal to 40 percent of their yield stresses, displays a more ductile behavior compared to model 9-b whose bolts are pre-stressed equal to 70 percent of their yield stresses. Therefore, high pre-stressing has probably caused local stresses in location where the steel plates are connected to the concrete and the connection fails before it reaches its maximum capacity. Fig. (33).

The maximum stress in the medial bolts of the beam and the column are 240 and 210 Mpa, respectively.

By drawing and comparing the separation contours of models 9-a and 5 which are the most ductile ones, it can be seen that at the final moment, the straps and the transverse stiffeners have adequately limited the slippage of the steel plates (Fig. 34).
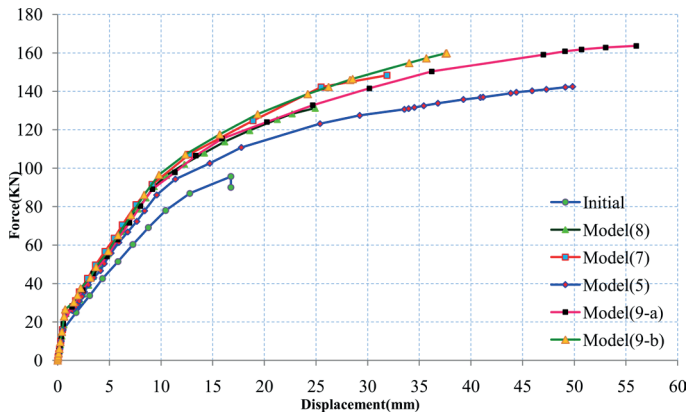
Fig. 33 Comparison between the load-displacement diagrams of model 9 and the other models
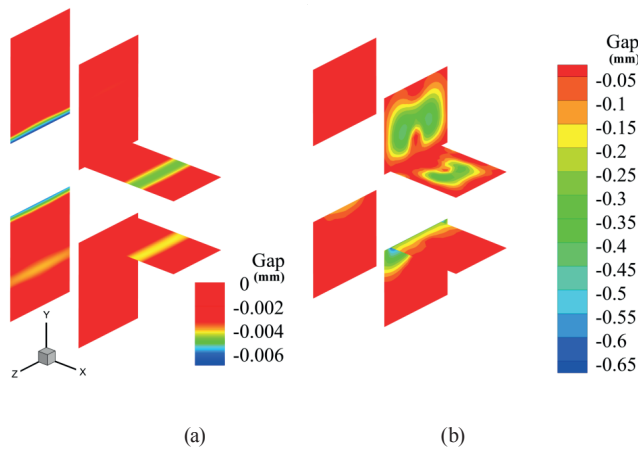

Fig. 35 (a) Von Mises stress contours of the reinforcing plates at the final moment of loading, (b) Strain diagram along the height of strap 3 at the final moment

Fig. 34 Comparing the separation at the final moment of load carrying in models 9-a (a) and 5 (b)

Fig. 36 The development location of the plastic hinge and the stress in the tensile and compressive steel bars at the location of the plastic hinge

By drawing the Von Mises stress contours of the steel plates at the final moment, it can be seen that the straps are on the verge of yielding and with sufficient strain, have provided the connection with enough ductility. As it can be observed in Fig. (35), an area of both the straps 2 and 3 have yielded but the straps are still carrying load. By drawing the Von Mises strain distribution along the height of strap 3 at its final moment of load carrying, it is seen that the end sections of the straps have yielded right at the time the connection has reached its maximum capacity.

By drawing the critical force existing in the tensile steel bars of the beam, it is revealed that the location of the plastic hinge has been shifted 600 mm from the front of the column towards the inside of the beam which attests to the desirable behavior of this reinforcement (Fig. 36).
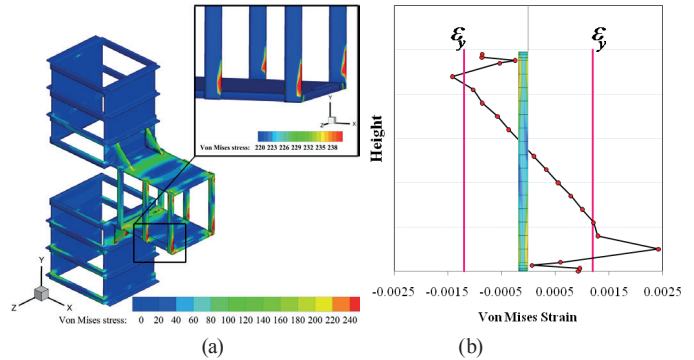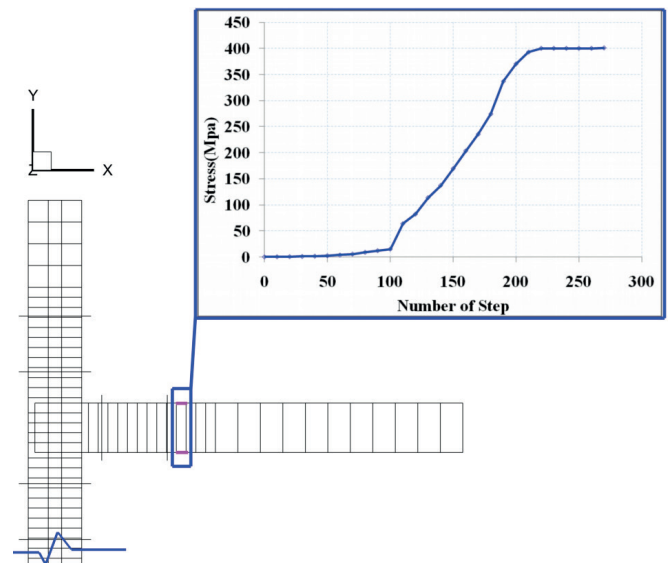
Usually the aim in reinforcement is increasing strength and providing ductility. By drawing the diagram, the percentage of the relative increase in the strength of the sample against its ductility will become quite evident. Model 9-a has displayed a desirable behavior and is suitable for retrofitting the connection. In comparison to the other models, this model not only increases the strength of the connection, it also meaningfully increases its ductility. It is worth mentioning that the FEMA 440 guideline was used to obtain the quasi-ductility criterion of the models. The load-displacement diagram was first bilinearized and then the ratio of the final displacement over the

Table 5 Relative strength percentages and the quasi ductility values of the models

Initial		Model 1		Model 2		Model 3		Model 4		Model 5		Model 6		Model 7		Model 8		Model 9-a		Model 9-b	
Strength	Quasi ductility	Strength	Quasi ductility	Strength	Quasi ductility	Strength	Quasi ductility	Strength	Quasi ductility	Strength	Quasi ductility	Strength	Quasi ductility	Strength	Quasi ductility	Strength	Quasi ductility	Strength	Quasi ductility	Strength	Quasi ductility
-	1.5	34.5	2.67	28.5	2.4	30.6	2.7	26.4	2.76	46.5	2.7	52.8	2.45	55	2.4	39.8	2.44	71	30.11	67.2	2.45

final displacement of the linear phase was used as the quasi-ductility of the connection. Table (4) presents the relative strength increase and the quasi-ductility values.

Using steel cages, G. Compione [41], reached 140 percent of relative strength increase in his best retrofitting model (C2RR). But his model was not initially imperfect. In the steel cage method, the concrete is not drilled. However, welding the side L-shaped profiles to the side straps seems difficult. The welding operation in model 9 is a lot more minor than the one carried out in model C2RR. Also, the existence of the medial bolts in model 9 causes the confinement stress in the concrete to increase and raises the strength of the connection. Thus, given the discussed investigations, the performance of the model can be considered desirable. Finally, given the fact the all the desirable and undesirable factors of the previous models have been taken under consideration in model 9, it is a suitable choice for retrofitting the connection.

7 Conclusions

The improper implementation of beam-column connections in in-situ reinforced concrete buildings is known to be one of the most important weak points with the potential of failure in reinforced concrete moment frames subjected to seismic loads. So, the present work investigates the performance of the imperfect concrete beam-column connection by proposing 9 reinforcing models to improve the behavior of the connection.

In the initial model, with the destruction of the concrete of the defective area and the buckling of the steel bars, the beam-column connection has become unstable. Therefore, retrofitting the connection seems imperative. Through a step-by-step approach, it was probed how different parameters can influence the behaviour of a retrofitting scheme and finally, based on the results of the analyses, a suitable and optimal model was proposed. This methodology can provide the engineer with a good understanding of the effects of the parameters affecting a retrofitting scheme. An overview of the results from all the reinforcing models are is as follows:

- In model 1, steel plates with the width of 450 mm, the same width as the beam and column, were attached to the beam and column using 2 medial bolts that were pre-stressed equal to 40 percent of their yield stress. The reinforcement caused 34 percent strength increase and brought about a displacement of 41 mm.
- In model 2, to increase the confinement stress of the concrete, the pre-stressing of the bolts was increased to 70 percent of their yield stress.
- In model 3, considering that the medial tensile bolts did not reach their maximum bearable stress, the diameter of the bolts was attenuated from 20 mm to 18 mm which from financial and material use standpoints was beneficial. Also, by comparing different pre-stressings of the bolts, it was concluded that increasing the pre-stressing

of the bolts causes stress concentration at the location of the holes and also brings about local failure.

- In model 4, by omitting the medial tensile bolts and connecting the steel plates with three unpre-stressed bolts, only the effect of the friction between the steel plates and the concrete was assessed. By investigating the separation of the plate, it was observed that separation does not occur at the sides of the plates. Thus, the simultaneous use of medial and side bolts would possibly yield better results.
- In model 5, the reinforcing plates were annexed to the beam and column using medial bolts pre-stressed equal to 70 percent of their stress and side bolts with no pre-stressing. The effect of the simultaneous use of medial and side bolts is pretty obvious. The strength of the connection has increased by 46 percent and the displacement has increased by 50 mm.
- In model 6, the reinforcing plates were attached to the beam and column using side and medial bolts. All the bolts in this model were pre-stressed equal to 70 percent of their yield stresses. Increased initial stiffness is quite clear in this model. However, ductility has decreased. The reason behind this is the support-like behavior of the concrete covering resulted from the tension of the side bolts which causes local failure and low ductility in this model.
- In model 7, to find the optimum length of the plate and also to drive the plastic hinge away from the front of the column, the length of the column was increased to 950 mm. A 55 percent increase in strength and a displacement of 33 mm are quite clear. Also, by investigating the stresses of the reinforcing plates, it became evident that the ending 300 mm portion of the plate has a very small share in load carrying and therefore removing it in model 9 seemed sound from the financial and material use standpoints.
- In model 8, the effects of adding transverse stiffeners to level out the stresses resulted from the initial pre-stressing of the medial bolts and also decreasing the angle of the triangular stiffeners were investigated. By investigating the separation of the plate from the concrete, it can be seen that adding transverse stiffeners is very effective. Also, decreasing the angle of the triangular stiffeners reduces the initial stiffness which is not desirable. This model increases the strength of the connection by 40 percent and causes a displacement of 33 mm.
- Model 9 is a combination of all the other models and takes into account their advantages and deficiencies. In this model, the medial bolts were pre-stressed equal to 40 percent and 70 percent of the bolts' yield stresses. It was observed that the model whose bolts are pre-stressed equal to 40 percent of their yield stresses displays a far more ductile behavior compared to the one whose bolts are pre-stressed equal to 70 percent of their yield stresses. This model increases the strength of the connection by

71 percent and brings about a displacement of 57 mm. In this model, the plate has a length of 650 mm and has the same width as the beam and the column. To transfer the stress resulted from the initial pre-stressing of the medial bolts of the column, three transverse stiffeners were used. To prevent the support-like behavior of the side bolts, straps were utilized in place of bolts. By assessing the stress of the medial bolts at the final moment, it was discovered that their stresses are far from the failure limit and therefore their performance was suitable. Aside from some small areas in the corners, stress in the side straps at the final moment of loading did not reach the yield stress. Also, by increasing the length of the plate and creating a good connection between the reinforcing plates and the concrete, the plastic hinge was driven away from the front of the column and was created at a distance between 650 to 700 mm away from connection.

Ultimately, it seems that to retrofit weak or defective connections, all the necessary measures regarding retrofitting techniques have to be taken under consideration and the effects of all the influencing factors have to be studied so that by discovering and observing the positive aspects of each influencing factor, the best retrofitting model could be chosen.

References

[1] Park, R., Paulay, T. "*Reinforced concrete structures*". John Wiley & Sons. 1975:

[2] Paulay, T., Priestly, M. "Frontmatter". In: *Seismic Design of Reinforced Concrete and Masonry Buildings*. John Wiley & Sons, Inc., Hoboken, NJ, USA. fmatter Wiley Online Library. 2009. 10.1002/9780470172841

[3] Moehle, J. P., Mahin, S. A. "Observations on the behavior of reinforced concrete buildings during earthquakes". *Special Publication*, 127, pp. 67–90. 1991.

[4] Kam, W.Y., Pampanin, S, Elwood, K. "Seismic performance of reinforced concrete buildings in the 22 February Christchurch (Lyttelton) earthquake". *Bulletin of the New Zealand Society for Earthquake Engineering*, 44(4), pp. 239–278. 2011. http://hdl.handle.net/10092/9006

[5] Doğangün, A. "Performance of reinforced concrete buildings during the May 1, 2003 Bingöl Earthquake in Turkey". *Engineering Structures*, 26(6), pp. 841–856. 2004. 10.1016/j.engstruct.2004.02.005

[6] Ghobarah, A., Saatcioglu, M., Nistor, I. "The impact of the 26 December 2004 earthquake and tsunami on structures and infrastructure". *Engineering Structures*, 28(2), pp. 312–326. 2006. 10.1016/j.engstruct.2005.09.028

[7] Turel Gur, AliCihan Pay, Julio A. Ramirez, Mete A. Sozen, Arvid M. Johnson, Ayhan Irfanoglu, Antonio Bobet. "Performance of School Buildings in Turkey During the 1999 Düzce and the 2003 Bingöl Earthquakes". *Earthquake Spectra*, 25(2), pp. 239–256. 2009. 10.1193/1.3089367

[8] Zhao, B., Taucer, F., Rossetto, T. "Field investigation on the performance of building structures during the 12 May 2008 Wenchuan earthquake in China". *Engineering Structures*, 31(8), pp. 1707–1723. 2009. 10.1016/j.engstruct.2009.02.039

[9] Sezen, H., Whittaker, A. S., Elwood, K. J., Mosalam, K. M. "Performance of reinforced concrete buildings during the August 17, 1999 Kocaeli, Turkey earthquake, and seismic design and construction practise in Turkey". *Engineering Structures*, 25(1), pp. 103–114. 2003. 10.1016/S0141-0296(02)00121-9

[10] Miller, D. K. "Lessons learned from the Northridge earthquake". *Engineering Structures*, 20(4–6), pp. 249–260. 1988. 10.1016/S0141-0296(97)00031-X

[11] Sezen, H. "Repair and Strengthening of Reinforced Concrete Beam-Column Joints with Fiber-Reinforced Polymer Composites". *Journal of Composites for Construction*, 16(5), pp. 499–506. 2012. 10.1061/(ASCE)CC.1943-5614.0000290

[12] Cheung, P. C., Paulay, T., Park, R. "New Zealand tests on full-scale reinforced concrete beam-column-slab subassemblages designed for earthquake resistance". *Special Publication*, 123, pp. 1–38. 1991.

[13] Dhakal, R. P., Pan, T.-C., Irawan, P., Tsai, K.-C., Lin, K.-C., Chen, C.-H. "Experimental study on the dynamic response of gravity-designed reinforced concrete connections". *Engineering Structures*, 27(1): p. 75–87. 2005. 10.1016/j.engstruct.2004.09.004

[14] Pantelides, C. P., Clyde, C., Reaveley, L. D. "Performance-Based Evaluation of Reinforced Concrete Building Exterior Joints for Seismic Excitation". *Earthquake Spectra*, 18(3), pp. 449–480. 2002. 10.1193/1.1510447

[15] Hakuto, S., Park, R., Tanaka, H. "Seismic Load Tests on Interior and Exterior Beam-Column Joints with Substandard Reinforcing Details". *Structural Journal*, 97(1), pp. 11–25, 2000. 10.14359/829

[16] Beres, A., Pessiki, S. P., White, R. N., Gergely, P. "Implications of Experiments on the Seismic Behavior of Gravity Load Designed RC Beam-to-Column Connections". *Earthquake Spectra*, 12(2), pp. 185–198. 1996. 10.1193/1.1585876

[17] Zhu, B., Chen, Y. "Behavior of Exterior Reinforced Concrete Beam Column Joints Subjected to Bi-Directional Cyclic Loading". *Special Publication*, 123. 1991.

[18] Alcocer, S. M., Jirsa, J. O. "Strength of reinforced concrete frame connections rehabilitated by jacketing". *ACI Structural Journal*, 90(3), pp. 249–261. 1993.

[19] Pimanmas, A., Chaimahawan, P. "Shear strength of beam–column joint with enlarged joint area". *Engineering structures*, 32(9), pp. 2529–2545. 2010. 10.1016/j.engstruct.2010.04.021

[20] Tsonos, A. G. "Lateral load response of strengthened reinforced concrete beam-to-column joints". *ACI Structural Journal*, 1999. 96(1), pp. 46–56. 1999. 10.14359/595

[21] Tsonos, A.-D. G.. "Performance enhancement of R/C building columns and beam–column joints through shotcrete jacketing". *Engineering Structures*, 32(3), pp. 726–740. 2010. 10.1016/j.engstruct.2009.12.001

[22] Karayannis, C. G., Chalioris, C. E., Sirkelis, G. M. "Local retrofit of exterior RC beam–column joints using thin RC jackets—An experimental study". *Earthquake Engineering & Structural Dynamics*, 37(5), pp. 727–746. 2008. 10.1002/eqe.783

[23] Bracci, J. M., Reinhorn, A.M., Mander, J. B. "Seismic retrofit of reinforced concrete buildings designed for gravity loads: performance of structural model". *ACI Structural Journal*, 92(6), pp. 711–723. 1995. 10.14359/9665

[24] Ghobarah, A., Aziz, T. S., Biddah, A. "Seismic Rehabilitation of Reinforced Concrete Beam-Column Connections". *Earthquake Spectra*, 12(4), pp. 761–780. 1996. 10.1193/1.1585909

[25] Ghobarah, A., Said, A. "Shear strengthening of beam-column joints". *Engineering Structures*, 24(7), pp. 881–888. 2002. 10.1016/S0141-0296(02)00026-3

[26] Engindeniz, M., Kahn, L. F., Abdul-Hamid, Z. "Repair and strengthening of reinforced concrete beam-column joints: State of the art". *ACI structural journal*, 102(2), pp. 187–197. 2005. 10.14359/14269

[27] Shafaei, J., Hosseini, A., Marefat, M. S. "Seismic retrofit of external RC beam–column joints by joint enlargement using prestressed steel angles". *Engineering Structures*, 81, pp. 265–288. 2014. 10.1016/j.engstruct.2014.10.006

[28] Pampanin, S., Christopoulos, C., Chen, T.-H. "Development and valida-
tion of a metallic haunch seismic retrofit solution for existing under-de-
signed RC frame buildings". *Earthquake Engineering & Structural Dy-
namics*, 35(14), pp. 1739–1766. 2006. 10092/214

[29] Said, A., Nehdi, M. "Rehabilitation of RC frame joints using local steel
bracing". *Structure and Infrastructure Engineering*, 4(6), pp. 431–447.
2006. 10.1080/15732470600822033

[30] Brunesi, E., Nascimbene, R., Rassati, G. A. "Seismic response of MRFs
with partially-restrained bolted beam-to-column connections through FE
analyses". *Journal of Constructional Steel Research*, 107, pp. 37–49.
2015. https://doi.org/10.1016/j.jcsr.2014.12.022

[31] Brunesi, E., Nascimbene, R., Rassati, G. A. "Response of partially-re-
strained bolted beam-to-column connections under cyclic loads". *Jour-
nal of Constructional Steel Research*, 97, pp. 24–38. 2014. https://doi.
org/10.1016/j.jcsr.2014.01.014

[32] Chaimahawan, P., Pimanmas, A. "Seismic retrofit of substandard beam-
column joint by planar joint expansion". *Materials and Structures*, 42(4),
pp. 443–459. 2009. 10.1617/s11527-008-9393-7

[33] Yurdakul, Ö., Avşar, Ö. "Strengthening of substandard reinforced concrete
beam-column joints by external post-tension rods". *Engineering Struc-
tures*, 107, pp. 9–22. 2016. 10.1016/j.engstruct.2015.11.004

[34] Arzeytoon, A., Hosseini, A., Goudarzi, A. "Seismic Rehabilitation of Ex-
terior RC Beam-Column Joints Using Steel Plates, Angles, and Postten-
sioning Rods". *Journal of Performance of Constructed Facilities*, 30(1),
p. 04014200. 2014. 10.1061/(ASCE)CF.1943-5509.0000721

[35] Shafaei, J., Hosseini, A., Marefat, M. S., Ingham, J. M. "Rehabilitation of
earthquake damaged external RC beam-column joints by joint enlarge-
ment using prestressed steel angles". *Earthquake Engineering & Struc-
tural Dynamics*, 46(2), pp. 291–316. 2017. 10.1002/eqe.2794

[36] Youssef, N. F., Bonowitz, D., Gross, J. L. "A survey of steel moment-
resisting frame buildings affected by the 1994 Northridge earthquake". US
National Institute of Standards and Technology. 1995.

[37] Venture, S.J., *Interim guidelines: evaluation, repair, modification and de-
sign of steel moment frames*. Rep. No. SAC 95, 1995. 2.

[38] Yu, Q.-S., Uang, C.-M., Gross, J. "Seismic rehabilitation design of steel
moment connection with welded haunch". *Journal of Structural Engineer-
ing*, 126(1), pp. 69–78. 2000. 10.1061/(ASCE)0733-9445(2000)126:1(69)

[39] Uang, C.-M., Yu, Q.-S., Noel, S., Gross, J. "Cyclic testing of steel mo-
ment connections rehabilitated with RBS or welded haunch". *Journal of
Structural Engineering*, 126(1), pp. 57–68. 2000. 10.1061/(ASCE)0733-
9445(2000)126:1(57)

[40] Willam, K., Warnke, E. "Constitutive model for the triaxial behavior of
concrete". In: *Proceedings, international association for bridge and struc-
tural engineering*. ISMES, Bergamo, Italy. 1975.

[41] Santarsiero, G., Masi, A. "Seismic performance of RC beam–column
joints retrofitted with steel dissipation jackets". *Engineering Structures*,
85, pp. 95–106. 2015. 10.1016/j.engstruct.2014.12.013

[42] Brunesi, E., Nascimbene, R., Rassati, G. A. „Seismic response of MRFs
with partially-restrained bolted beam-to-column connections through FE
analyses". *Journal of Constructional Steel Research*, 107, pp. 37–49.
2015. https://doi.org/10.1016/j.jcsr.2014.12.022

[43] Rabbat, B. G., Russell, H. „ Friction coefficient of steel on concrete or
grout". *Journal of Structural Engineering*, 111(3), pp. 505–515. 10.1061/
(ASCE)0733-9445(1985)111:3(505)